

Unearthing the soil carbon food web with DNA-SIP

Ashley N Campbell * †, Charles Pepe-Ranney * ‡, and Daniel H Buckley ‡

*co-first author, †Department of Microbiology, Cornell University, New York, USA, and ‡Department of Crop and Soil Sciences, Cornell University, New York, USA

Submitted to Proceedings of the National Academy of Sciences of the United States of America

Abstract

We describe an approach for identifying microbial contributions to soil C cycling using nucleic acid stable isotope probing (SIP) coupled with next generation sequencing. ^{13}C -xylose or ^{13}C -cellulose were chosen to carry the isotopic label for DNA-SIP. Microcosm DNA was interrogated for ^{13}C incorporation at days 1, 3, 7, 14 and 30. Incorporation of ^{13}C from xylose into microcosm DNA was observed at days 1, 3, and 7, while incorporation of ^{13}C from cellulose peaked at day 14 and was maintained through day 30. From approximately 6,000 OTUs detected, a total of 49 and 63 unique OTUs assimilated ^{13}C from xylose and cellulose into DNA, respectively. Xylose assimilating OTUs were more abundant in the microcosm community than cellulose assimilating OTUs, while cellulose OTUs demonstrated a greater substrate specificity than xylose OTUs.

Significance

We have limited understanding of soil carbon (C) cycling dynamics despite the fact that the terrestrial biosphere contains a large fraction of the global C pool. Microbial processes are responsible for the majority of soil C cycling but have proven difficult to study due to the wide range of organisms participating in C reactions. Using a mixture of C substrates, we identified temporal C use dynamics in discrete soil microbial taxa. This sheds light on the soil microbial community transitions associated with the biomass degradation process and is the first ever demonstration of simultaneously tracking distinct C substrate use dynamics of multiple C substrates through a soil microbial community *ex situ*. Furthermore, we identified novel microorganisms involved in the decomposition of cellulose, the most abundant biopolymer globally. Application of this method may help to identify microbial taxa that mediate soil C cycling and increase our understanding of soil C use dynamics.

monolayer | structure | x-ray reflectivity | molecular electronics

Abbreviations: SAM, self-assembled monolayer; OTS, octadecyltrichlorosilane

Introduction

Excluding plant biomass, there are 2,300 Pg of carbon (C) stored in soils worldwide which accounts for ~80% of the global terrestrial C pool [1, 2]. When organic C from plants reaches soil it is degraded by fungi, archaea, and bacteria. The majority of plant biomass C in soil is respiration and produces 10 times more CO_2 annually than anthropogenic emissions [3]. Global changes in atmospheric CO_2 , temperature, and ecosystem nitrogen inputs are expected to impact soil C input [4]. Current climate change models concur on atmospheric and oceanic but not terrestrial C predictions [5]. Contrasting terrestrial C model predictions reflect how little is known about soil C cycling. Inconsistencies in terrestrial modeling could be improved by elucidating the relationship between dissolved organic C and soil microbial community composition [6].

An important step in understanding soil C cycling dynamics is identifying the *in situ* activity of specific microbial lineages to establish the relationship between community structure and function [7]. An estimated 80-90% of soil C cycling is mediated by microorganisms [8, 9] but understanding microbial processing of soil nutrients is challenging due to soil's heterogeneous nature and methods limitations. The vast majority of microorganisms resist cultivation in the laboratory. Stable-isotope probing (SIP) links microbial identity and activity without cultivation and has expanded our knowledge of microbial contributions to biogeochemical processes [10]. The most successful applications of SIP have identified organisms which mediate processes performed by a nar-

Reserved for Publication Footnotes

row set of functional guilds such as methanogens [11]. SIP has been less applicable to the study of soil C cycling because of limitations in resolving power as a result of simultaneous labeling of many different organisms in the community. Additionally, molecular applications such as tRFLP, DGGE and cloning that are frequently used in conjunction with SIP provide insufficient resolution of taxon identity and/or depth of coverage. We developed an approach called **High Resolution-SIP** (HR-SIP) that employs a complex mixture of substrates added to soil at a low concentration relative to soil organic matter pools along with high throughput DNA sequencing. This greatly expands the ability of nucleic acid SIP to explore complex patterns of C-cycling in microbial communities with increased resolution.

A temporal activity cascade occurs in natural microbial communities during plant biomass degradation in which labile C is degraded before polymeric C [12, 13]. The aim of this study was to observe temporal dynamics of C assimilation through discrete soil community members. Our experimental approach included the addition of a soil organic matter (SOM) simulant (a complex mixture of model carbon sources and inorganic nutrients common to plant biomass) to soil microcosms where a single C component is substituted for its ^{13}C -labeled equivalent. Parallel incubations of soils amended with this complex C mixture allows us to observe how different C substrates move through the soil microbial community. In this study we used ^{13}C -xylose and ^{13}C -cellulose as a proxy for labile and polymeric C, respectively, and coupled nucleic acid stable isotope probing with high throughput DNA sequencing. Amplicon sequencing of 16S rRNA gene fragments from many gradient fractions and multiple gradients make it possible to track C associated activities for hundreds of soil taxa.

Results

We observed C use dynamics in an agricultural soil microbial community by conducting a nucleic acid SIP experiment wherein xylose or cellulose carried the isotopic label. We set up three soil microcosm series. Each microcosm was amended with a C substrate mixture that included cellulose and xylose. The C substrate mixture approximated the chemical composition of fresh plant biomass. The same mixture was added to microcosms in each series, however, for each series except the control, xylose or cellulose was substituted for its ^{13}C counterpart. Microcosm amendments are shorthand identified in figures by the following code: “ $^{13}\text{CXPS}$ ” refers to the amendment with ^{13}C -xylose (that is ^{13}C Xylose Plant Simulant), “ $^{13}\text{CCPS}$ ” refers to

the ^{13}C -cellulose amendment and “ $^{12}\text{CCPS}$ ” refers to the amendment that only contained ^{12}C substrates (i.e. control). 5.3 mg of C gram $^{-1}$ soil C substrate mixture was added to each microcosm representing 18% of the soil C. The mixture included 0.42 mg xylose-C and 0.88 mg cellulose-C g soil $^{-1}$. Microcosms were harvested at days 1, 3, 7, 14 and 30 during a 30 day incubation. ^{13}C -xylose assimilation peaked immediately and tapered over the 30 day incubation whereas ^{13}C -cellulose assimilation peaked two weeks after amendment additions (Figure 1).

See Supplemental Note XX for sequencing and density fractionation statistics.

Soil microcosm microbial community changes with time. Bulk soil DNA SSU rRNA gene amplicon sequencing revealed changes in the soil microcosm microbial community structure and membership correlated significantly with incubation time (Figure S8B, p-value 0.23, R^2 0.63, Adonis test [14]). The identity of the ^{13}C -labeled substrate added to the microcosms did not significantly correlate with community structure and membership (p-value 0.35). Additionally, microcosm beta diversity was significantly less than gradient fraction beta diversity (p-value 0.003, “betadisper” function R Vegan package [15, 16]). Twenty-nine OTUs significantly changed in relative abundance with time (“BH” adjusted p-value <0.10 , [17]) (Figure S3). OTUs that significantly increased in relative abundance with time included OTUs in the *Verrucomicrobia*, *Proteobacteria*, *Planctomycetes*, *Cyanobacteria*, *Chloroflexi* and *Actinobacteria*. OTUs that significantly decreased in relative abundance with time included OTUs in the *Proteobacteria*, *Firmicutes*, *Bacteroidetes* and *Actinobacteria* (Figure S3). *Proteobacteria* was the only phylum that had OTUs which increased significantly and OTUs that decreased significantly in abundance with time. If sequences were grouped by taxonomic annotations at the class level, only four classes significantly changed in abundance, *Bacilli* (decreased), *Flavobacteria* (decreased), *Gammaproteobacteria* (decreased) and *Herpetosiphonales* (increased) (Figure S6). Of the 29 OTUs that changed significantly in relative abundance with time, 14 are labeled substrate responders (see , Figure S3).

Responder abundances summed at phylum level generally increased for ^{13}C -cellulose (Figure S9) whereas ^{13}C -xylose responder abundances summed at the phylum level decreased over time for *Firmicutes*, *Bacteroidetes*, *Actinobacteria* and *Proteobacteria* although *Proteobacteria* spiked at day 14 (Figure S9). Bulk abundance trends are roughly consistent with ^{13}C assimilation.

OTUs that assimilated ^{13}C into DNA. Within the first 7 days of incubation approximately 63% of ^{13}C -xylose was respiration and only an additional 6% more was respiration from day 7 to 30. At day 30, 30% of the ^{13}C from xylose remained. An average 16% of the ^{13}C -cellulose added was respiration within the first 7 days, 38% by day 14, and 60% by day 30.

Isotope incorporation by an OTU is revealed by enrichment of the OTU in heavy CsCl gradient fractions containing ^{13}C labeled DNA relative to heavy fractions from control gradients containing no ^{13}C labeled DNA. We refer to OTUs that putatively incorporated ^{13}C into DNA originally from an isotopically labeled substrate as substrate “responders”. At day 1, 84% of ^{13}C -xylose responsive OTUs belonged to *Firmicutes*, 11% to *Proteobacteria* and 5% to *Bacteroidetes*. *Firmicutes* responders decreased from 16 OTUs at day 1 to one OTU at day 3 while *Bacteroidetes* responders increased from one OTU at day 1 to 12 OTUs at day 3. The remaining day 3 responders are members of the *Proteobacteria* (26%) and the *Verrucomicrobia* (5%). Day 7 responders were 53% *Actinobacteria*, 40% *Proteobacteria*, and 7% *Firmicutes*. The identities of ^{13}C -xylose responders changed with time. The numerically dominant ^{13}C -xylose responder phylum shifted from *Firmicutes* to *Bacteroidetes* and then to *Actinobacteria* across days 1, 3 and 7 (Figure S1, Figure 2).

Only 2 and 5 OTUs had incorporated ^{13}C from ^{13}C -cellulose at days 3 and 7, respectively. At days 14 and 30 42 and 39 OTUs incorporated ^{13}C from ^{13}C -cellulose into biomass. A *Cellvibrio* and *Sandaracinaceae* OTU assimilated ^{13}C from ^{13}C -cellulose at day 3. Day 7 ^{13}C -cellulose responders included the same *Cellvibrio* responder as day 3, a *Verrucomicrobia* OTU and three *Chloroflexi* OTUs. 50% of Day 14 responders belong to *Proteobacteria* (66% Alpha-, 19% Gamma-, and 14% Beta-) followed by 17% *Planctomycetes*, 14% *Verrucomicrobia*, 10% *Chloroflexi*, 7% *Actinobacteria* and 2% cyanobacteria. *Bacteroidetes* OTUs began to incorporate ^{13}C from cellulose at day 30 (13% of day 30 responders). Other day 30 responding phyla included *Proteobacteria* (30% of day 30 responders; 42% Alpha-, 42% Delta, 8% Gamma-, and 8% Beta-), *Planctomycetes* (20%), *Verrucomicrobia* (20%), *Chloroflexi* (13%) and cyanobacteria (3%). *Proteobacteria*, *Verrucomicrobia*, and *Chloroflexi* had relatively high numbers of responders with strong response across multiple time points (Figure S1).

Ecological strategies of ^{13}C responders. ^{13}C -xylose responders are generally more abundant members based on relative abundance in bulk DNA SSU rRNA gene content than ^{13}C -cellulose responders

(Figure 3, p-value 0.00028). However, both abundant and rare OTUs responded to ^{13}C -xylose and ^{13}C -cellulose (Figure 3). For instance, a *Deltaproteobacteria* ^{13}C -cellulose responder is fairly abundant in the bulk samples (“OTU.5”, Table S1). OTU.5 was on average the 13th most abundant OTU in bulk samples. A ^{13}C -xylose responder (“OTU.1040”, Table S2) has a mean relative abundance in bulk samples of 3.57×10^{-5} . Two ^{13}C -cellulose responders were not found in any bulk samples (“OTU.862” and “OTU.1312”, Table S1). Of the 10 most abundant responders, 8 are ^{13}C -xylose responders and 6 of these 8 are consistently among the 10 most abundant OTUs in bulk samples.

Cellulose responders exhibited a greater shift in buoyant density (BD) than xylose responders in response to isotope incorporation (Figure 3, p-value 1.8610x $^{-6}$). ^{13}C -cellulose responders shifted on average 0.0163 g mL^{-1} (sd 0.0094) whereas xylose responders shifted on average 0.0097 g mL^{-1} (sd 0.0094). For reference, 100% ^{13}C DNA BD is 0.04 g mL^{-1} greater than the BD of its ^{12}C counterpart. DNA BD increases as its ratio of ^{13}C to ^{12}C increases. An organism that only assimilates C into DNA from a ^{13}C isotopically labeled source, will have a greater $^{13}\text{C}:^{12}\text{C}$ ratio in its DNA than an organism utilizing a mixture of isotopically labeled and unlabeled C sources (see supplemental note XX).

^{13}C -xylose responder estimated *rrn* gene copy number was inversely related time of first response (p-value 2.02×10^{-15} , Figure S2). OTUs that first respond at later time points have fewer estimated *rrn* copy number than OTUs that first respond earlier (Figure S2).

Discussion

Pure culture based studies have historically driven soil microbial ecology research but cultured isolates have not captured *in situ* numerically abundant genera [18]. DNA-SIP can characterize functional roles for thousands of phylotypes in a single experiment without cultivation. We identified 104 OTUs in an agricultural soil that incorporated ^{13}C from xylose and/or cellulose into biomass and characterized substrate specificity and C-cycling dynamics for these soluble and polymeric C degraders. Included in ^{13}C -xylose and ^{13}C -cellulose responsive OTUs were members of cosmopolitan yet functionally uncharacterized soil phylogenetic groups such as *Verrucomicrobia*, *Planctomycetes* and *Chloroflexi*.

Microbial response to isotopic labels. We propose that C added to soil microcosms in this experiment took the following path through the microbial food web (Figure S13): First, labile C such as

xylose was assimilated by fast-growing opportunistic *Firmicutes* spore formers. The remaining labile C and new biomass C was assimilated in succession by slower growing *Bacteroidetes*, *Actinobacteria* and *Proteobacteria* phylotypes that were either tuned to lower C substrate concentrations, were predatory bacteria (e.g. *Agromyces*), and/or were specialized for consuming viral lysate. C from polymeric substrates entered the bacterial community after 14 days. Canonical cellulose degrading bacteria such as *Cellvibrio* degraded cellulose but uncharacterized lineages in the *Chloroflexi*, *Planctomycetes* and *Verrucomicrobia*, specifically the *Spartobacteria*, were also significant contributors to cellulose decomposition.

Ecological strategies of soil microorganisms participating in the decomposition of organic matter.

We assessed the ecology of ^{13}C -responsive OTUs by estimating the *rrn* gene copy number and the BD shift upon labeling for each OTU. *rrn* gene copy number correlates positively with growth rate [19] and BD shift is indicative of substrate specificity (see results). Ecological metrics suggest ^{13}C -cellulose responsive OTUs grow slower (Figure 3, Figure S2), have greater substrate specificity (Figure 3), and are generally lower abundance than ^{13}C -xylose responsive OTUs (Figure 3). The higher abundance of xylose responders may also be in part due to of their high *rrn* gene copy number resulting in inflated relative abundance per genome. There are only faint ecological differences within the ^{13}C -cellulose responsive OTUs but the combination of *rrn* gene copy number, BD shift, abundance rank and relative abundance change over time is consistent with phylum membership (Figure RADVIZ). ^{13}C -xylose responsive OTU *rrn* gene copy number correlated inversely with the time at which the OTU was first found to incorporate ^{13}C into DNA (Figure 3, Figure S2) suggesting that fast-growing microbes assimilated ^{13}C from xylose before slow growers.

Labile C responder ecological strategies were more varied than polymeric ecological strategies perhaps because some ^{13}C labeled microorganisms did not primarily assimilate xylose but became labeled via predatory interactions and/or are saprophytes. It's not clear whether the observed activity succession from *Firmicutes* to *Bacteroidetes* and finally *Actinobacteria* in response to ^{13}C -xylose addition marks a trophic cascade or functional groups tuned to different resource concentrations or both. Notably, each temporally defined response group clustered phylogenetically suggesting a uniform ecological strategy (Figure S7). It's also clear that some of the non-*Firmicutes* ^{13}C -xylose responders are closely related to known predators (*Agromyces*) and many marine predatory bacte-

ria are members of the *Bacteroidetes* ([20]). Further, *Bacteroidetes* have been previously implicated as soil predatory bacteria [21]. If the temporal dynamics of ^{13}C -xylose incorporation are due to trophic interactions, our results suggest that there are many predatory soil bacteria that consume fast-growing, opportunistic, primary labile C assimilating, gram-positive spore-formers. Hence, trophic interactions among soil bacteria may be of importance in soil C turnover models.

How – or if – phylogenetic composition affects SOM dynamics is an open question [22]. It is likely that the ability to carry out soil C transformations are redundant within and between soil microbial communities and that in the mineral soil abiotic factors are rate limiting [22]. Therefore, phylogenetic composition in mineral soil likely influences soil C fate as opposed to dynamics. We demonstrate a phylogenetically coherent response with time to soluble C additions – for instance, most of the initial response to xylose can be attributed to aerobic spore formers from few related genera. Assuming cellular resource allocation is consistent with phylogeny, it follows then that phylogenetic composition can significantly influence SOM fate. Polymeric C did not show the same phylogenetic coherence as soluble C decomposition in this study. This suggests that resource allocation among cellulose degraders would not have a single phylogenetic signal and the fate of polymeric C would not be similarly tied to phylogenetic composition.

Conclusion. Microorganisms sequester atmospheric C and respire soil organic matter (SOM) influencing climate change on a global scale but we do not know which microorganisms carry out specific soil C transformations. In this experiment microbes from uncharacterized yet ubiquitous soil lineages participated in cellulose decomposition. Cellulose C degraders included members of the *Verrucomicrobia* (*Spartobacteria*), *Chloroflexi*, *Bacteroidetes* and *Planctomycetes*. *Spartobacteria* in particular globally cosmopolitan soil microorganisms and often the most abundant *Verrucomicrobia* order in soil CITE. Our results also suggest that members of the *Bacteroidetes* and *Actinobacteria* act in the cascade of labile, soluble C through soil trophic levels possibly as predators. Both points illustrate the complexity of soil C dynamics and fate. The largely phylogenetically coherent ecological groups observed in this study suggest that soil C fate is tied to phylogenetic composition.

Methods

Additional information on sample collection and analytical methods is provided in SI Materials and Methods.

Twelve soil cores (5 cm diameter x 10 cm depth) were collected from six random sampling locations within an organically managed agricultural field in Penn Yan, New York. Soils were pretreated by sieving (2 mm), homogenizing sieved soil, and pre-incubating 10 g of dry soil weight in flasks for 2 weeks. Soils were amended with a 5.3 mg g soil⁻¹ carbon mixture; representative of natural concentrations [23]. Mixture contained 38% cellulose, 23% lignin, 20% xylose, 3% arabinose, 1% galactose, 1% glucose, and 0.5% mannose by mass, with the remaining 13.5% mass composed of an amino acid (in-house made replica of Teknova C0705) and basal salt mixture (Murashige and Skoog, Sigma Aldrich M5524). Three parallel treatments were performed; (1) unlabeled control,(2)¹³C-cellulose, (3)¹³C-xylose (98 atom% ¹³C, Sigma Aldrich). Each treatment had 2 replicates per time point (n = 4) except day 30 which had 4 replicates; total microcosms per treatment n = 12, except ¹³C-cellulose which was not sampled at day 1, n = 10. Other details relating to substrate addition can be found in SI. Microcosms were sampled destructively (stored at -80°C until nucleic acid processing) at days 1 (control and xylose only), 3, 7, 14, and 30.

Nucleic acids were extracted using a modified Griffiths protocol [24]. To prepare nucleic acid extracts for isopycnic centrifugation as previously described [25], DNA was size selected (>4kb) using 1% low melt agarose gel and β -agarase I enzyme extraction per manufacturers protocol (New England Biolab, M0392S). For each time point in the series isopycnic gradients were setup using a modified protocol [26] for a total of five ¹²C-control, five ¹³C-xylose, and four ¹³C-cellulose microcosms. A density gradient (average density 1.69 g mL⁻¹) solution of 1.762 g cesium chloride (CsCl) mL⁻¹ in gradient buffer solution (pH 8.0 15 mM Tris-HCl, 15 mM EDTA, 15 mM KCl) was used to separate ¹³C-enriched and ¹²C-nonenriched DNA. Each gradient was loaded with approximately 5 μ g of DNA and ultracentrifuged for 66 h at 55,000 rpm and room temperature (RT). Fractions of ~100 μ L were collected from below by displacing the DNA-CsCl-gradient buffer solution in the centrifugation tube with water using a syringe pump at a flow rate of 3.3 μ L s⁻¹ [27] into AcroprepTM 96 filter plate (Pall Life Sciences 5035). The refractive index of each fraction was measured using a Reichert AR200 digital refractometer modified as previously described [25] to measure a volume of 5 μ L. Then buoyant density was calculated from the refractive index as previously described [25] (see also SI). The collected DNA fractions were purified by repetitive washing of Acroprep filter wells with TE. Finally, 50 μ L TE was added to each fraction then resus-

pended DNA was pipetted off the filter into a new microfuge tube.

For every gradient, 20 fractions were chosen for sequencing between the density range 1.67-1.75 g mL⁻¹. Barcoded 454 primers were designed using 454-specific adapter B, 10 bp barcodes [28], a 2 bp linker (5'-CA-3'), and 806R primer for reverse primer (BA806R); and 454-specific adapter A, a 2 bp linker (5'-TC-3'), and 515F primer for forward primer (BA515F). Each fraction was PCR amplified using 0.25 μ L 5 U μ l⁻¹ AmpliTaq Gold (Life Technologies, Grand Island, NY; N8080243), 2.5 μ L 10X Buffer II (100 mM Tris-HCl, pH 8.3, 500 mM KCl), 2.5 μ L 25 mM MgCl₂, 4 μ L 5 mM dNTP, 1.25 μ L 10 mg mL⁻¹ BSA, 0.5 μ L 10 μ M BA515F, 1 μ L 5 μ M BA806R, 3 μ L H₂O, 10 μ L 1:30 DNA template) in triplicate. Samples were normalized either using Pico green quantification and manual calculation or by SequalPrepTM normalization plates (Invitrogen, Carlsbad, CA; A10510), then pooled in equimolar concentrations. Pooled DNA was gel extracted from a 1% agarose gel using Wizard SV gel and PCR clean-up system (Promega, Madison, WI; A9281) per manufacturer's protocol. Amplicons were sequenced on Roche 454 FLX system using titanium chemistry at Selah Genomics (formerly EnGenCore, Columbia, SC)

References

1. Amundson R (2001) The carbon budget in soils. *Annu Rev Earth Planet Sci* 29(1): 535–562.
2. Batjes N-H (1996) Total carbon and nitrogen in the soils of the world. *European Journal of Soil Science* 47(2): 151–163.
3. Chapin F (2002) Principles of terrestrial ecosystem ecology.
4. Groenigen K-J, Graaff M-A, Six J, Harris D, Kuikman P, Kessel C (2006) The impact of elevated atmospheric CO₂ on soil C and N dynamics: a meta-analysis. *Managed Ecosystems and CO₂* (Springer Science, Berlin Heidelberg), pp 373–391.
5. Friedlingstein P, Cox P, Betts R, Bopp L, von W-B, Brovkin V, et al. (2006) Climate–carbon cycle feedback analysis: Results from the C4 mip model intercomparison. *J Climate* 19(14): 3337–3353.
6. Neff J-C, Asner G-P (2001) Dissolved organic carbon in terrestrial ecosystems: synthesis and a model. *Ecosystems* 4(1): 29–48.
7. O'Donnell A-G, Seasman M, Macrae A, Waite I, Davies J-T (2002) Plants and fertilisers as drivers of change in microbial community structure and function in soils. *Interactions in the Root Environment: An Integrated Ap-*



- proach (Springer, Netherlands), pp 135–145.
- 8. Coleman D-C, Crossley D-A (1996) Fundamentals of Soil Ecology.
 - 9. Nannipieri P, Ascher J, Ceccherini M-T, Landi L, Pietramellara G, Renella G (2003) Microbial diversity and soil functions. *European Journal of Soil Science* 54(4): 655–670.
 - 10. Chen Y, Murrell J-C (2010) When metagenomics meets stable-isotope probing: progress and perspectives. *Trends Microbiol* 18(4): 157–163.
 - 11. Lu Y (2005) In situ stable isotope probing of methanogenic archaea in the rice rhizosphere. *Science* 309(5737): 1088–1090.
 - 12. Hu S, van Bruggen A-HC (1997) Microbial dynamics associated with multiphasic decomposition of ^{14}C -Labeled Cellulose in Soil. *Microb Ecol* 33(2): 134–143.
 - 13. Rui J, Peng J, Lu Y (2009) Succession of bacterial populations during plant residue decomposition in rice field soil. *Appl Environ Microbiol* 75(14): 4879–4886.
 - 14. Anderson M-J (2001) A new method for non-parametric multivariate analysis of variance. *Austral Ecology* 26(1): 32–46.
 - 15. Anderson M-J, Ellingsen K-E, McArdle B-H (2006) Multivariate dispersion as a measure of beta diversity. *Ecology Letters* 9(6): 683–693.
 - 16. Oksanen J, Kindt R, Legendre P, OHara B, Stevens M-HH, Oksanen M-J, et al. (2007) The vegan package.
 - 17. Benjamini Y, Hochberg Y (1995) Controlling the false discovery rate: a practical and powerful approach to multiple testing. *Journal of the Royal Statistical Society, Series B* 57(1): 289–300.
 - 18. Janssen P-H (2006) Identifying the dominant soil bacterial taxa in libraries of 16S rRNA and 16S rRNA genes. *Appl Environ Microbiol* 72(3): 1719–1728.
 - 19. Klappenbach J, Saxman P, Cole J, Schmidt T (2001) rrndb: the Ribosomal RNA Operon Copy Number Database.. *Nucleic Acids Res* 29(1): 181–184.
 - 20. Banning E-C, Casciotti K-L, Kujawinski E-B (2010) Novel strains isolated from a coastal aquifer suggest a predatory role for flavobacteria. *FEMS Microbiol Ecol* 73(2): 254–270.
 - 21. Lueders T, Kindler R, Miltner A, Friedrich M-W, Kaestner M (2006) Identification of bacterial micropredators distinctively active in a soil microbial food web. *Appl Environ Microbiol* 72(8): 5342–5348.
 - 22. Schimel J-P, Schaeffer S-M (2012) Microbial control over carbon cycling in soil. *Frontiers in Microbiology* 3: 348. doi: 10.3389/fmicb.2012.00348
 - 23. Schneckenberger K, Demin D, Stahr K, Kuzyakov Y (2008) Microbial utilization and mineralization of ^{14}C glucose added in six orders of concentration to soil. *Soil Biology and Biochemistry* 40(8): 1981–1988.
 - 24. Griffiths R-I, Whiteley A-S, O'Donnell A-G, Bailey M-J (2000) Rapid method for coextraction of DNA and RNA from natural environments for analysis of ribosomal DNA- and rRNA-based microbial community composition. *Appl Environ Microbiol* 66(12): 5488–5491.
 - 25. Buckley D-H, Huangyutitham V, Hsu S-F, Nelson T-A (2007) Stable isotope probing with ^{15}N achieved by disentangling the effects of genome G+C content and isotope enrichment on dna Density. *Appl Environ Microbiol* 73(10): 3189–3195.
 - 26. Neufeld J-D, Vohra J, Dumont M-G, Lueders T, Manefield M, Friedrich M-W, et al. (2007) DNA stable-isotope probing. *Nature Protocols* 2(4): 860–866.
 - 27. Manefield M, Whiteley A-S, Griffiths R-I, Bailey M-J (2002) RNA Stable isotope probing a novel means of linking microbial community function to phylogeny. *Appl Environ Microbiol* 68(11): 5367–5373.
 - 28. Hamady M, Walker J-J, Harris J-K, Gold N-J, Knight R (2008) Error-correcting barcoded primers for pyrosequencing hundreds of samples in multiplex. *Nat Meth* 5(3): 235–237.

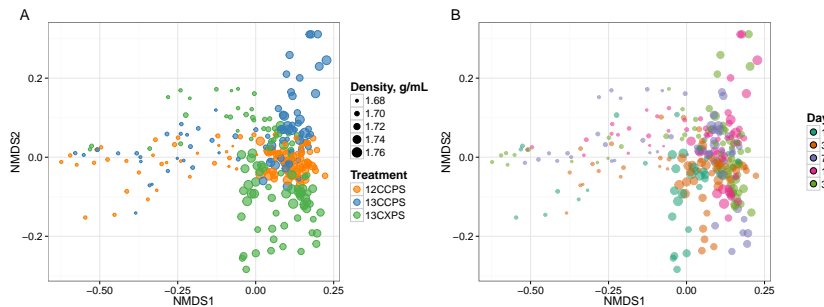


Fig. 1. NMDS analysis from weighted unifrac distances of 454 sequence data from SIP fractions of each treatment over time. Twenty fractions from a CsCl gradient fractionation for each treatment at each time point were sequenced (Fig. S1). Each point on the NMDS represents the bacterial composition based on 16S sequencing for a single fraction where the size of the point is representative of the density of that fraction and the colors represent the treatments (A) or days (B).

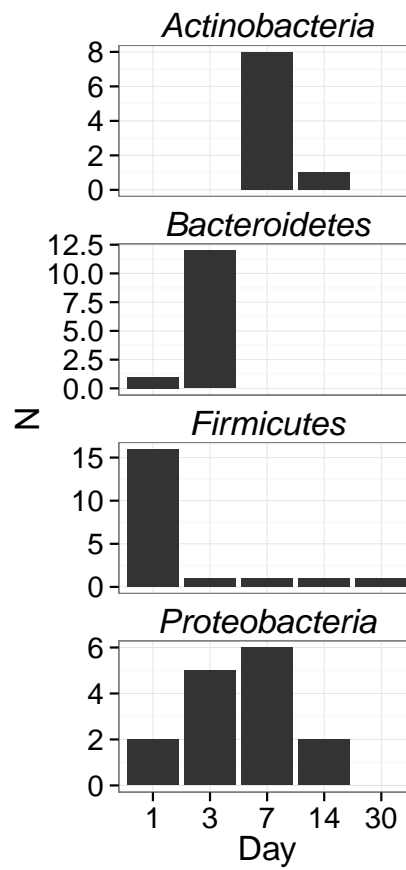


Fig. 2. Counts of ^{13}C -xylose responders in the *Actinobacteria*, *Bacteroidetes*, *Firmicutes* and *Proteobacteria* at days 1, 3, 7 and 30.

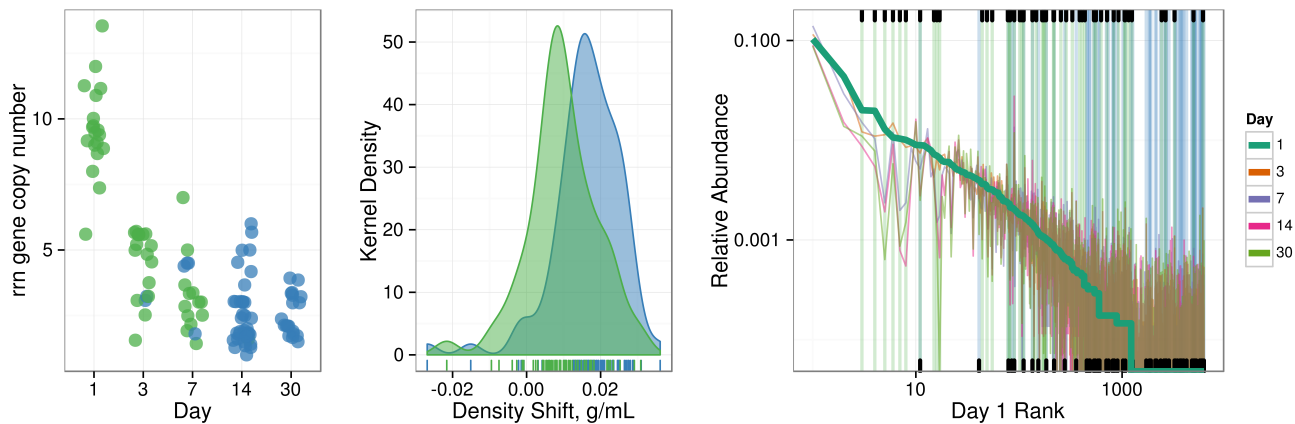


Fig. 3. ^{13}C -responder characteristics based on density shift (A) and rank (B). Kernel density estimation of ^{13}C -responder's density shift in cellulose treatment (blue) and xylose treatment (green) demonstrates degree of labeling for responders for each respective substrate. ^{13}C -responders in rank abundance are labeled by substrate (cellulose, blue; xylose, green). Ticks at top indicate location of ^{13}C -cytose responders in bulk community. Ticks at bottom indicate location of ^{13}C -cellulose responders in bulk community. OTU rank was assessed from day 1 bulk samples.

Supplemental Figures and Tables

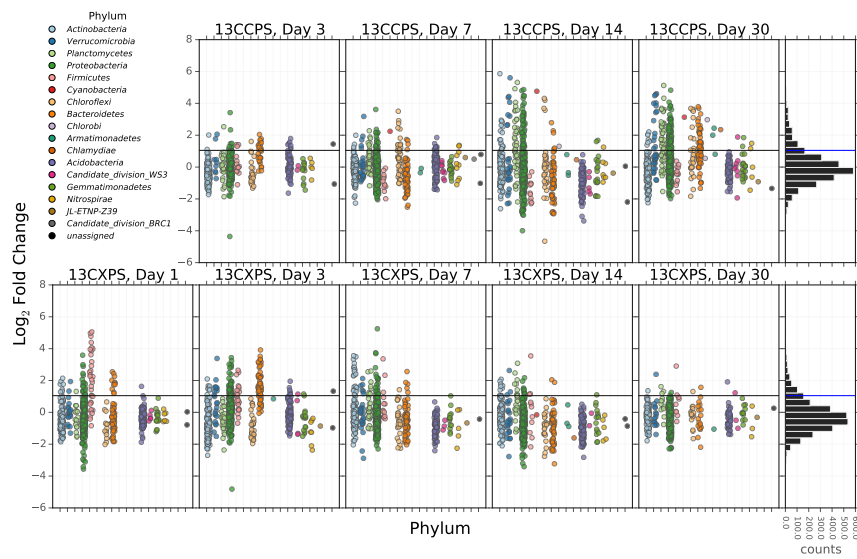


Fig. S1. Log₂ fold change of ¹³C-responders in cellulose treatment (top) and xylose treatment (bottom). Log₂ fold change is based on the relative abundance in the experimental treatment compared to the control within the density range 1.7125–1.755 g ml⁻¹. Taxa are colored by phylum. ‘Counts’ is a histogram of log₂ fold change values.

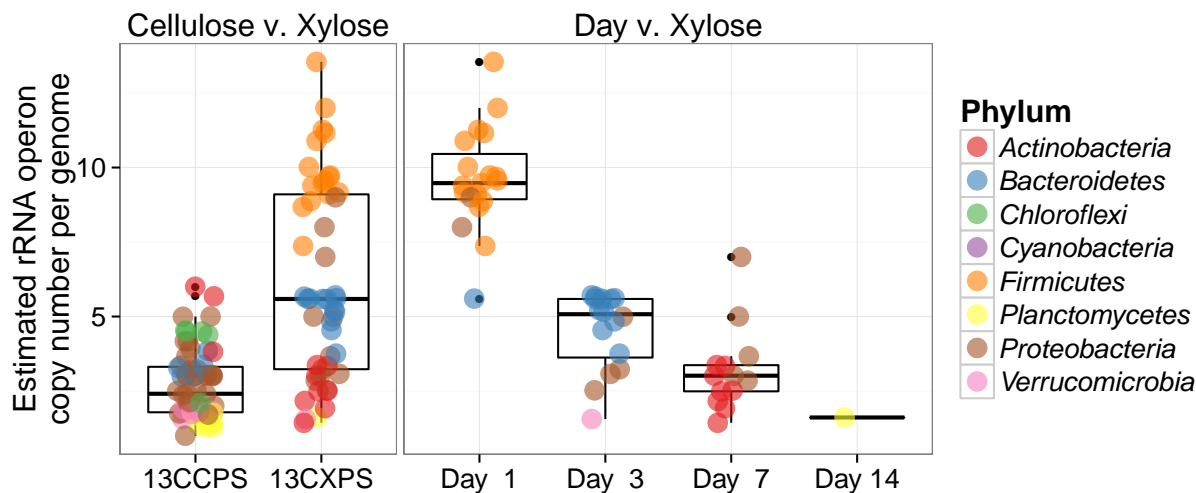


Fig. S2. Estimated rRNA operon copy number per genome for ¹³C responding OTUs. Panel titles indicate which labeled substrate(s) are depicted.

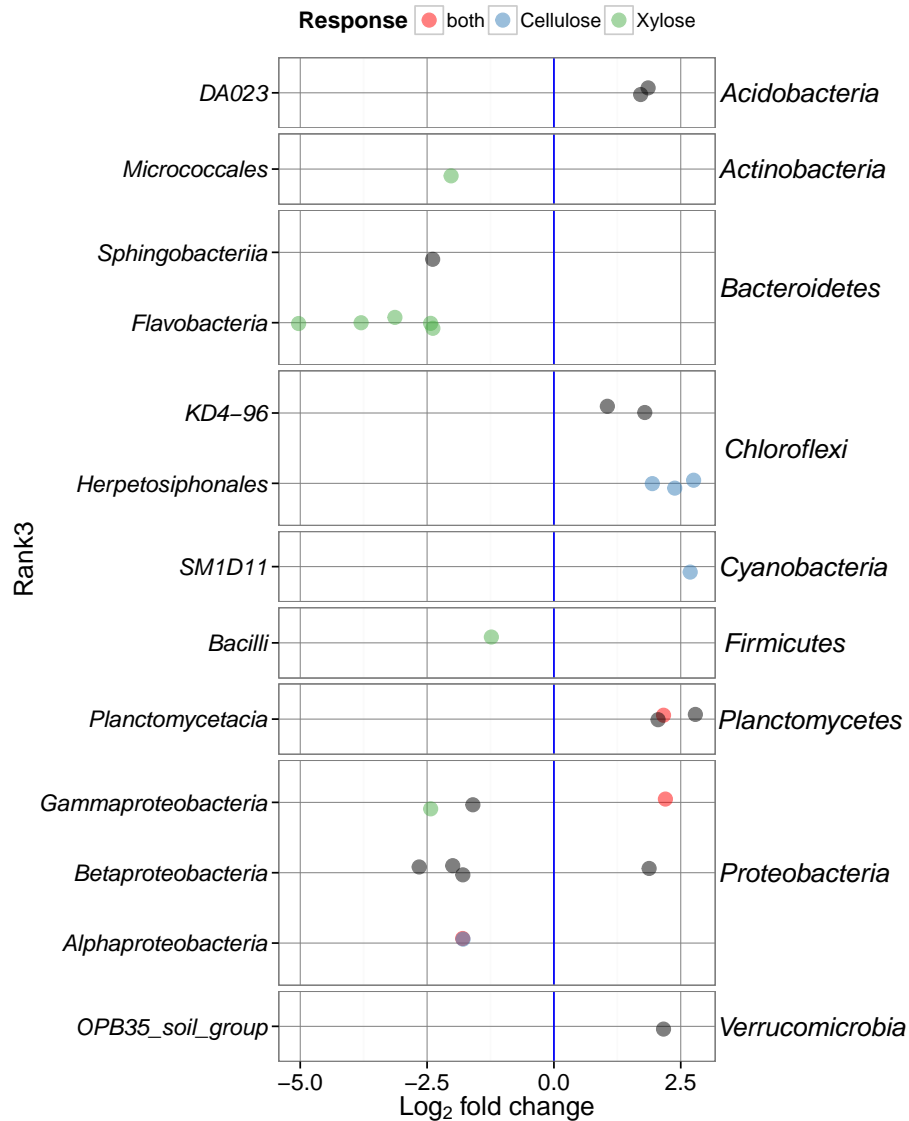


Fig. S3. Fold change time⁻¹ for OTUs that changed significantly in abundance over time. One panel per phylum (phyla indicated on the right). Taxonomic class indicated on the left.

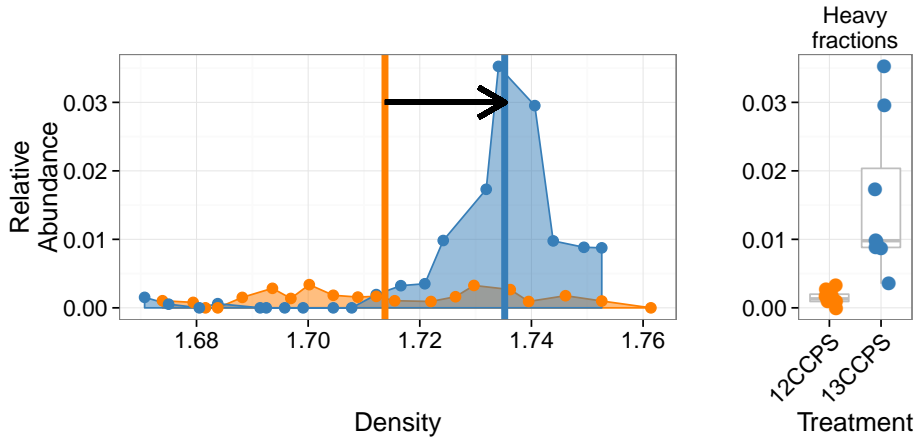


Fig. S4. Density profile for a single ^{13}C -cellulose “responder” OTU in the labeled gradient, blue, and the control gradient, orange. Vertical lines show center of mass for each density profile and arrow denotes the magnitude and direction of the BD shift upon labeling. Panel at right shows relative abundance values in the heavy fractions for each gradient.

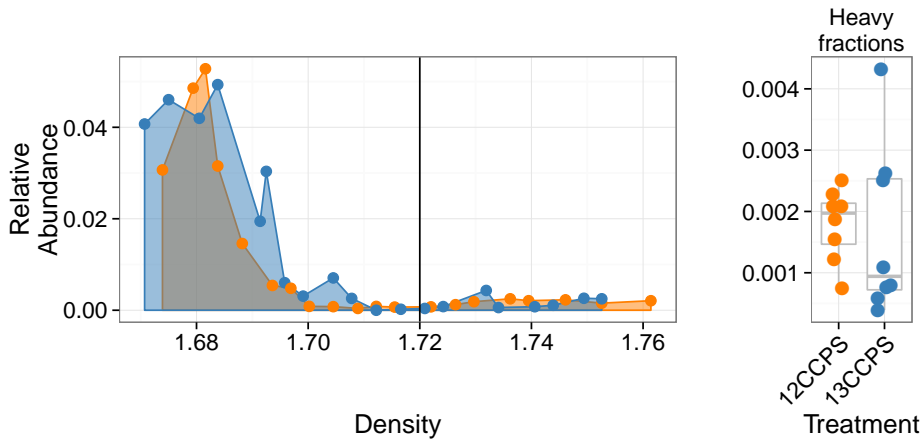


Fig. S5. Density profile for a single ^{13}C -cellulose “non-responder” OTU in the labeled gradient, blue, and the control gradient, orange. Vertical line shows where “heavy” fractions begin as defined in our analysis. Panel at right shows relative abundance values in the heavy fractions for each gradient.

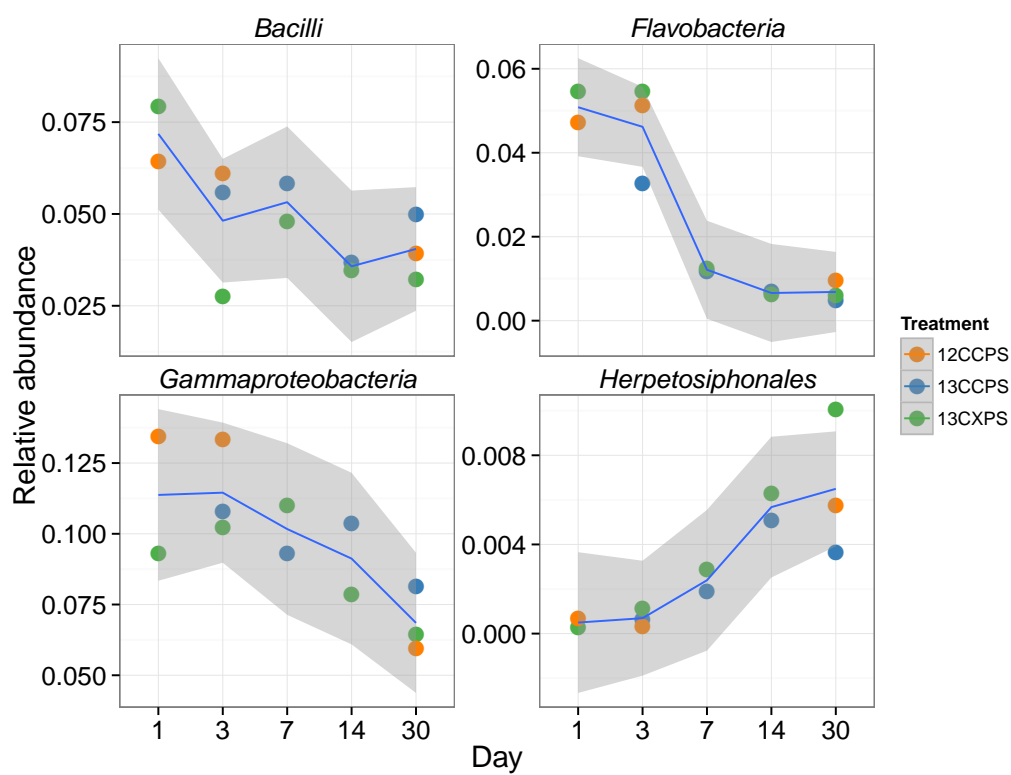


Fig. S6. Relative abundance versus day for classes that changed significantly in relative abundance with time.

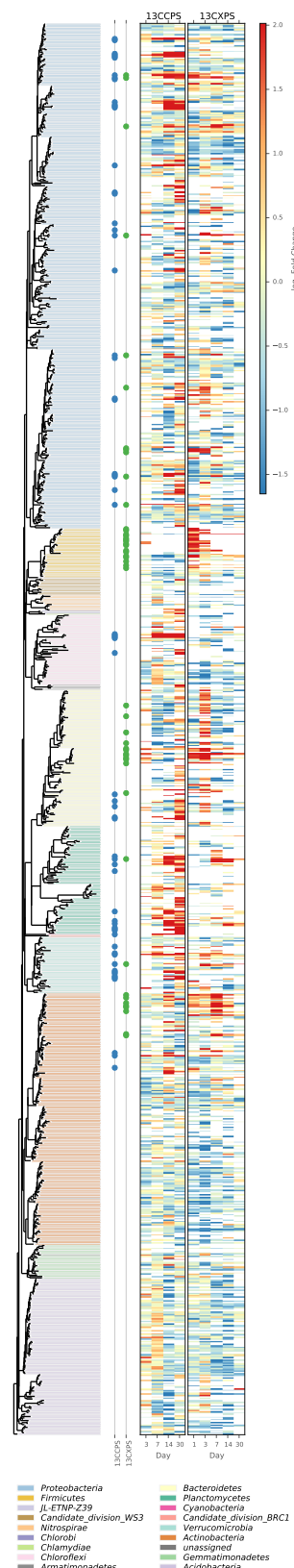


Fig. S7. Phylogenetic tree of sequences passing a user defined sparsity threshold (0.6) for at least one day of the time series. Branches are colored by phylum. ^{13}C -responders for cellulose (blue) and xylose (green) are indicated by a point beside the respective branch. Heatmap demonstrates \log_2 fold change of each taxa through the full time series for both treatments (cellulose, left; xylose, right).

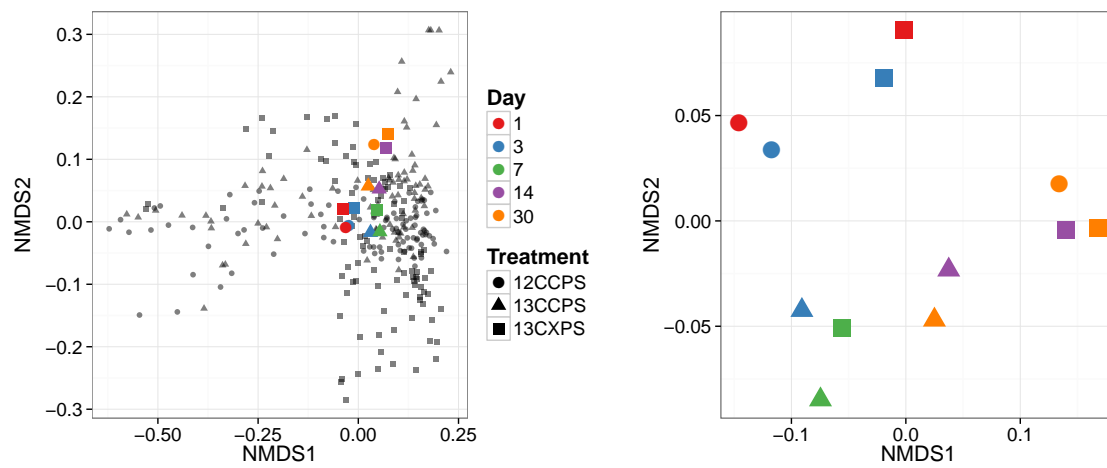


Fig. S8. Ordination of bulk gradient fraction phylogenetic profiles.

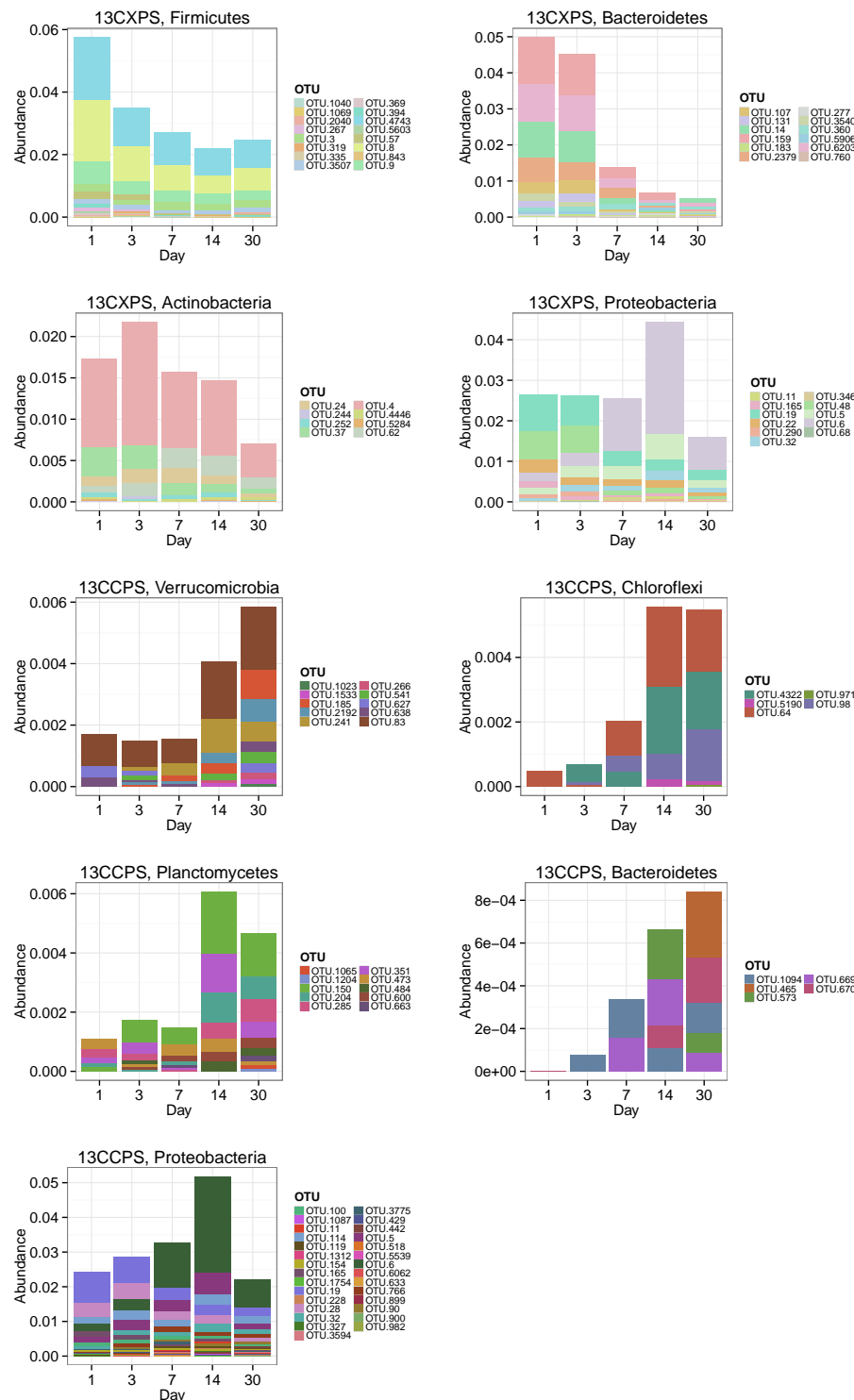


Fig. S9. Sum of bulk abundances with selected phylum for responder OTUs.

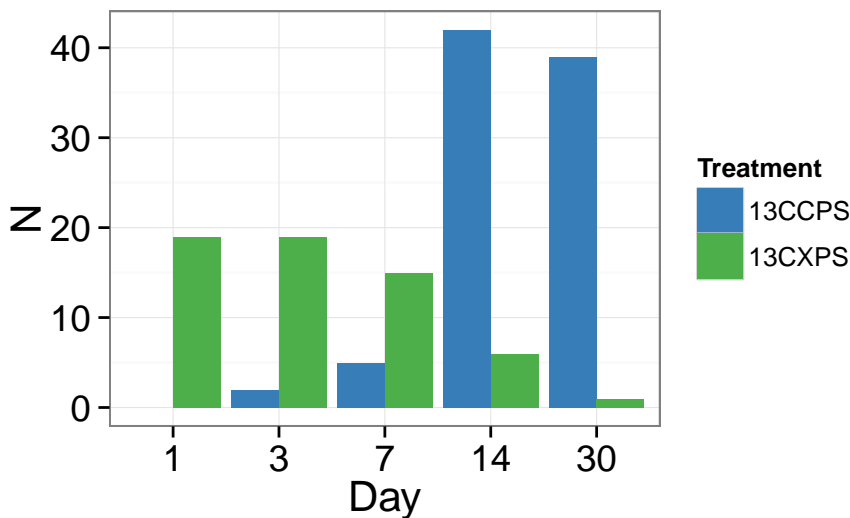


Fig. S10. Counts of responders to each isotopically labeled substrate (cellulose and xylose) over time.

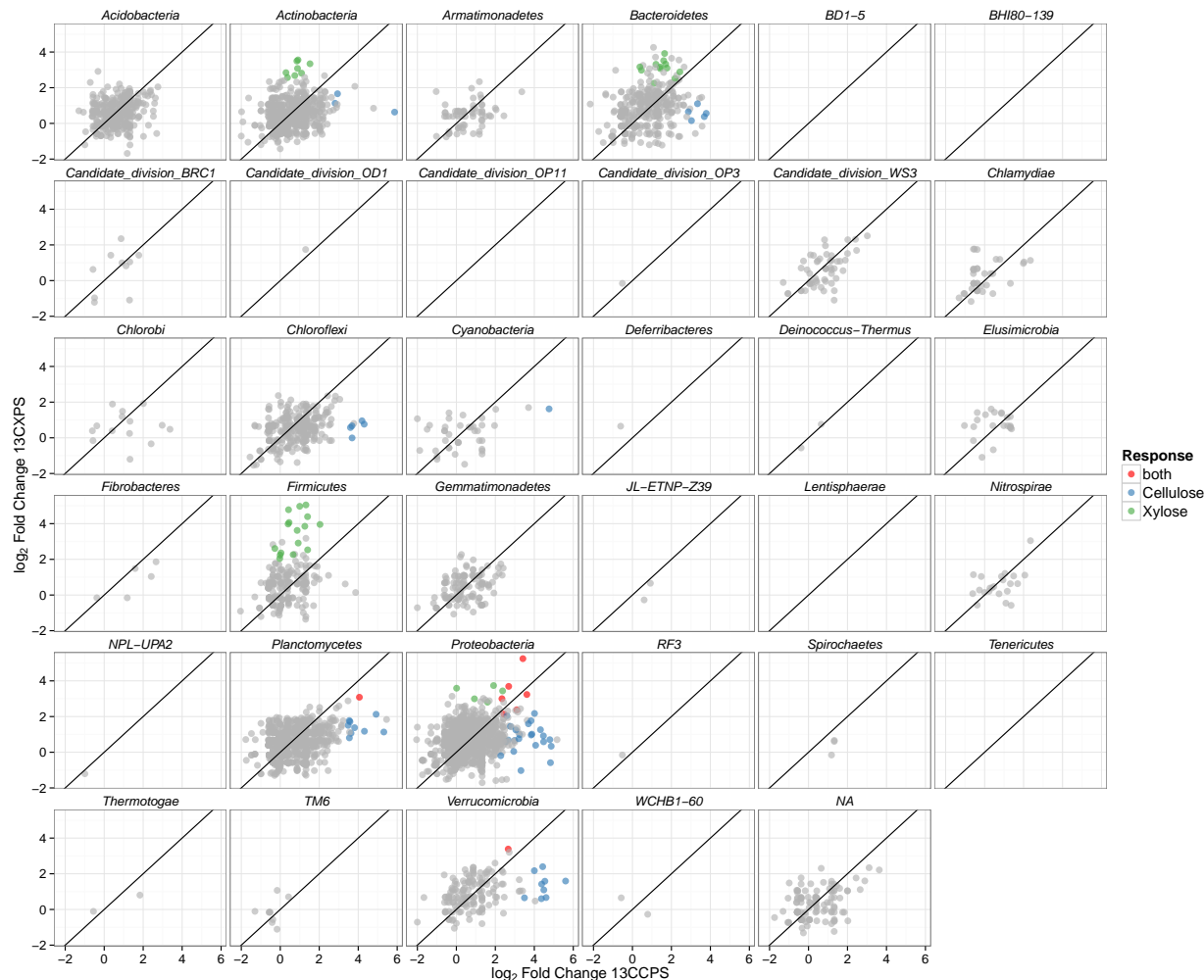


Fig. S11. Maximum \log_2 fold change in response to labeled substrate incorporation for each substrate and all OTUs that pass sparsity filtering in both substrate analyses. Points colored by response. Line has slope of 1 with intercept at the origin. OTUs falling in the top-right quadrant responded to both substrates while those in the top-left and bottom-right responded to ^{13}C -xylose and ^{13}C -cellulose, respectively.



Fig. S12. Phylum specific trees. Heatmap indicates fold change between heavy fractions of control gradients versus labeled gradients. Dots indicate the position of “responders” to ¹³C-xylose (green) or ¹³C-cellulose (blue).

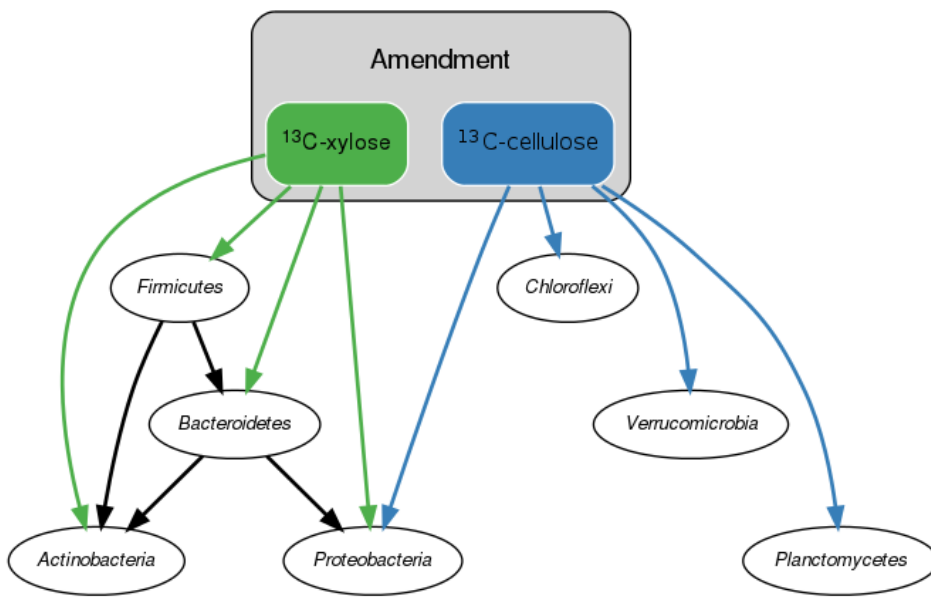


Fig. S13. Conceptual model of soil food web in this experiment.

Table S1: ¹³C-cellulose responders BLAST against Living Tree Project

OTU ID	Fold change ^a	Day ^b	Top BLAST hits	BLAST %ID	Phylum;Class;Order
OTU.862	5.87	14	<i>Allokutzneria albata</i>	100.0	<i>Actinobacteria Pseudonocardiales Pseudonocardiaceae</i>
OTU.257	2.94	14	<i>Lentzea waywayandensis, Lentzea flaviverrucosa</i>	100.0	<i>Actinobacteria Pseudonocardiales Pseudonocardiaceae</i>
OTU.132	2.81	14	<i>Streptomyces spp.</i>	100.0	<i>Actinobacteria Streptomycetales Streptomycetaceae</i>
OTU.465	3.79	30	<i>Ohtaekwangia kribbensis</i>	92.73	<i>Bacteroidetes Cytophagia Cytophagales</i>
OTU.1094	3.69	30	<i>Sporocytophaga myxococcoides</i>	99.55	<i>Bacteroidetes Cytophagia Cytophagales</i>
OTU.669	3.34	30	<i>Ohtaekwangia koreensis</i>	92.69	<i>Bacteroidetes Cytophagia Cytophagales</i>
OTU.573	3.03	30	<i>Adhaeribacter aerophilus</i>	92.76	<i>Bacteroidetes Cytophagia Cytophagales</i>
OTU.670	2.87	30	<i>Adhaeribacter aerophilus</i>	91.78	<i>Bacteroidetes Cytophagia Cytophagales</i>
OTU.971	3.68	30	No hits of at least 90% identity	78.57	<i>Chloroflexi Anaerolineae Anaerolineales</i>
OTU.64	4.31	14	No hits of at least 90% identity	89.5	<i>Chloroflexi Herpetosiphonales Herpetosiphonaceae</i>
OTU.4322	4.19	14	No hits of at least 90% identity	89.14	<i>Chloroflexi Herpetosiphonales Herpetosiphonaceae</i>
OTU.98	3.68	14	No hits of at least 90% identity	88.18	<i>Chloroflexi Herpetosiphonales Herpetosiphonaceae</i>
OTU.5190	3.6	30	No hits of at least 90% identity	88.13	<i>Chloroflexi Herpetosiphonales Herpetosiphonaceae</i>
OTU.120	4.76	14	<i>Vampirovibrio chlorellavorus</i>	94.52	<i>Cyanobacteria SM1D11 uncultured-bacterium</i>
OTU.1065	5.31	14	No hits of at least 90% identity	84.55	<i>Planctomycetes Planctomycetacia Planctomycetales</i>
OTU.484	4.92	14	No hits of at least 90% identity	89.09	<i>Planctomycetes Planctomycetacia Planctomycetales</i>
OTU.1204	4.32	30	<i>Planctomyces limnophilus</i>	91.78	<i>Planctomycetes Planctomycetacia Planctomycetales</i>
OTU.150	4.06	14	No hits of at least 90% identity	86.76	<i>Planctomycetes Planctomycetacia Planctomycetales</i>
OTU.663	3.63	30	<i>Pirellula staleyi DSM 6068</i>	90.87	<i>Planctomycetes Planctomycetacia Planctomycetales</i>
OTU.473	3.58	14	<i>Pirellula staleyi DSM 6068</i>	90.91	<i>Planctomycetes Planctomycetacia Planctomycetales</i>
OTU.285	3.55	30	<i>Blastopirellula marina</i>	90.87	<i>Planctomycetes Planctomycetacia Planctomycetales</i>
OTU.351	3.54	14	<i>Pirellula staleyi DSM 6068</i>	91.86	<i>Planctomycetes Planctomycetacia Planctomycetales</i>
OTU.600	3.48	30	No hits of at least 90% identity	80.37	<i>Planctomycetes Planctomycetacia Planctomycetales</i>
OTU.900	4.87	14	<i>Brevundimonas vesicularis, Brevundimonas nasdae</i>	100.0	<i>Proteobacteria Alphaproteobacteria Caulobacterales</i>
OTU.1754	4.48	14	<i>Asticcacaulis biprosthecum, Asticcacaulis benevestitus</i>	96.8	<i>Proteobacteria Alphaproteobacteria Caulobacterales</i>
OTU.119	3.31	14	<i>Brevundimonas alba</i>	100.0	<i>Proteobacteria Alphaproteobacteria Caulobacterales</i>

Table S1 – continued from previous page

OTU ID	Fold change	Day	Top BLAST hits	BLAST %ID	Phylum;Class;Order
OTU.327	2.99	14	<i>Asticcacaulis biprosthecum,</i> <i>Asticcacaulis benevestitus</i>	98.63	Proteobacteria Alphaproteobacteria Caulobacterales
OTU.982	4.47	14	<i>Devosia neptuniae</i>	100.0	Proteobacteria Alphaproteobacteria Rhizobiales
OTU.1087	4.32	14	<i>Devosia soli</i> , <i>Devosia crocina</i> , <i>Devosia riboflavina</i>	99.09	Proteobacteria Alphaproteobacteria Rhizobiales
OTU.5539	4.01	14	<i>Devosia subaequoris</i>	98.17	Proteobacteria Alphaproteobacteria Rhizobiales
OTU.3775	3.88	14	<i>Devosia glacialis</i> , <i>Devosia chinhatensis</i> , <i>Devosia geojensis</i> , <i>Devosia yakushimensis</i>	98.63	Proteobacteria Alphaproteobacteria Rhizobiales
OTU.429	3.7	30	<i>Devosia limi</i> , <i>Devosia psychrophila</i>	97.72	Proteobacteria Alphaproteobacteria Rhizobiales
OTU.766	3.21	14	<i>Devosia insulae</i>	99.54	Proteobacteria Alphaproteobacteria Rhizobiales
OTU.165	3.1	14	<i>Rhizobium skieniewicense</i> , <i>Rhizobium vignae</i> , <i>Rhizobium larrymoorei</i> , <i>Rhizobium alkalisolii</i> , <i>Rhizobium galegae</i> , <i>Rhizobium huautlense</i>	100.0	Proteobacteria Alphaproteobacteria Rhizobiales
OTU.28	2.59	14	<i>Rhizobium giardinii</i> , <i>Rhizobium tubonense</i> , <i>Rhizobium tibeticum</i> , <i>Rhizobium mesoamericanum CCGE 501</i> , <i>Rhizobium herbae</i> , <i>Rhizobium endophyticum</i>	99.54	Proteobacteria Alphaproteobacteria Rhizobiales
OTU.19	2.44	14	<i>Rhizobium alamii</i> , <i>Rhizobium mesosinicum</i> , <i>Rhizobium mongolense</i> , <i>Arthrobacter viscosus</i> , <i>Rhizobium sullae</i> , <i>Rhizobium yanglingense</i> , <i>Rhizobium loessense</i>	99.54	Proteobacteria Alphaproteobacteria Rhizobiales
OTU.90	2.94	14	<i>Sphingopyxis panaciterrae</i> , <i>Sphingopyxis chilensis</i> , <i>Sphingopyxis sp. BZ30</i> , <i>Sphingomonas sp.</i>	100.0	Proteobacteria Alphaproteobacteria Sphingomonadales
OTU.518	4.8	14	<i>Hydrogenophaga intermedia</i>	100.0	Proteobacteria Betaproteobacteria Burkholderiales
OTU.1312	4.07	30	<i>Paucimonas lemoignei</i>	99.54	Proteobacteria Betaproteobacteria Burkholderiales
OTU.114	2.78	14	<i>Herbaspirillum sp. SUEMI03</i> , <i>Herbaspirillum sp. SUEMI10</i> , <i>Oxalicibacterium solurbis</i> , <i>Herminiumonas fonticola</i> , <i>Oxalicibacterium hortii</i>	100.0	Proteobacteria Betaproteobacteria Burkholderiales
OTU.633	3.84	30	No hits of at least 90% identity	89.5	Proteobacteria Deltaproteobacteria Myxococcales
OTU.3594	3.83	30	<i>Chondromyces robustus</i>	90.41	Proteobacteria Deltaproteobacteria Myxococcales
OTU.442	3.05	30	<i>Chondromyces robustus</i>	92.24	Proteobacteria Deltaproteobacteria Myxococcales
OTU.228	2.54	30	<i>Sorangium cellulosum</i>	98.17	Proteobacteria Deltaproteobacteria Myxococcales

Table S1 – continued from previous page

OTU ID	Fold change	Day	Top BLAST hits	BLAST %ID	Phylum;Class;Order
OTU.899	2.28	30	<i>Enhygromyxa salina</i>	97.72	<i>Proteobacteria Deltaproteobacteria Myxococcales</i>
OTU.6	3.62	7	<i>Cellvibrio fulvus</i>	100.0	<i>Proteobacteria Gammaproteobacteria Pseudomonadales</i>
OTU.6062	4.83	30	<i>Dokdonella sp. DC-3, Luteibacter rhizovicinus</i>	97.26	<i>Proteobacteria Gammaproteobacteria Xanthomonadales</i>
OTU.154	3.24	14	<i>Pseudoxanthomonas mexicana, Pseudoxanthomonas japonensis</i>	100.0	<i>Proteobacteria Gammaproteobacteria Xanthomonadales</i>
OTU.100	2.66	14	<i>Pseudoxanthomonas sacheonensis, Pseudoxanthomonas dokdonensis</i>	100.0	<i>Proteobacteria Gammaproteobacteria Xanthomonadales</i>
OTU.1023	4.61	30	No hits of at least 90% identity	80.54	<i>Verrucomicrobia Spartobacteria Chthoniobacterales</i>
OTU.266	4.54	30	No hits of at least 90% identity	83.64	<i>Verrucomicrobia Spartobacteria Chthoniobacterales</i>
OTU.541	4.49	30	No hits of at least 90% identity	84.23	<i>Verrucomicrobia Spartobacteria Chthoniobacterales</i>
OTU.185	4.37	14	No hits of at least 90% identity	85.14	<i>Verrucomicrobia Spartobacteria Chthoniobacterales</i>
OTU.2192	3.49	30	No hits of at least 90% identity	83.56	<i>Verrucomicrobia Spartobacteria Chthoniobacterales</i>
OTU.1533	3.43	30	No hits of at least 90% identity	82.27	<i>Verrucomicrobia Spartobacteria Chthoniobacterales</i>
OTU.83	5.61	14	<i>Luteolibacter sp. CCTCC AB 2010415</i>	97.72	<i>Verrucomicrobia Verrucomicrobiae Verrucomicrobiales</i>
OTU.627	4.43	14	<i>Verrucomicrobiaceae bacterium DC2a-G7</i>	100.0	<i>Verrucomicrobia Verrucomicrobiae Verrucomicrobiales</i>
OTU.638	4.0	30	<i>Luteolibacter sp. CCTCC AB 2010415, Luteolibacter algae</i>	93.61	<i>Verrucomicrobia Verrucomicrobiae Verrucomicrobiales</i>

^a Maximum observed \log_2 of fold change.^b Day of maximum fold change.

Table S2: ^{13}C -xylose responders BLAST against Living Tree Project

OTU ID	Fold change ^a	Day ^b	Top BLAST hits	BLAST %ID	Phylum;Class;Order
OTU.4446	3.49	7	<i>Catenuloplanes niger</i> , <i>Catenuloplanes castaneus</i> , <i>Catenuloplanes atrovinosus</i> , <i>Catenuloplanes crispus</i> , <i>Catenuloplanes nepalensis</i> , <i>Catenuloplanes japonicus</i>	97.72	Actinobacteria Frankiales Nakamurellaceae
OTU.62	2.57	7	<i>Nakamurella flava</i>	100.0	Actinobacteria Frankiales Nakamurellaceae
OTU.24	2.81	7	<i>Cellulomonas aerilata</i> , <i>Cellulomonas humilata</i> , <i>Cellulomonas terrae</i> , <i>Cellulomonas soli</i> , <i>Cellulomonas xylinilytica</i>	100.0	Actinobacteria Micrococcales Cellulomonadaceae
OTU.4	2.84	7	<i>Agromyces ramosus</i>	100.0	Actinobacteria Micrococcales Microbacteriaceae
OTU.37	2.68	7	<i>Phycicola gilvus</i> , <i>Microterricola viridarii</i> , <i>Frigoribacterium faeni</i> , <i>Frondihabitans sp. RS-15</i> , <i>Frondihabitans australicus</i>	100.0	Actinobacteria Micrococcales Microbacteriaceae
OTU.5284	3.56	7	<i>Isoptericola nanjingensis</i> , <i>Isoptericola hypogaeus</i> , <i>Isoptericola variabilis</i>	98.63	Actinobacteria Micrococcales Promicromonosporaceae
OTU.252	3.34	7	<i>Promicromonospora thailandica</i>	100.0	Actinobacteria Micrococcales Promicromonosporaceae
OTU.244	3.08	7	<i>Cellulosimicrobium funkei</i> , <i>Cellulosimicrobium terreum</i>	100.0	Actinobacteria Micrococcales Promicromonosporaceae
OTU.760	2.89	3	<i>Dyadobacter hamtensis</i>	98.63	Bacteroidetes Cytophagia Cytophagales
OTU.14	3.92	3	<i>Flavobacterium oncorhynchi</i> , <i>Flavobacterium glycines</i> , <i>Flavobacterium succinicans</i>	99.09	Bacteroidetes Flavobacteria Flavobacteriales
OTU.6203	3.32	3	<i>Flavobacterium granuli</i> , <i>Flavobacterium glaciei</i>	100.0	Bacteroidetes Flavobacteria Flavobacteriales
OTU.159	3.16	3	<i>Flavobacterium hibernum</i>	98.17	Bacteroidetes Flavobacteria Flavobacteriales
OTU.2379	3.1	3	<i>Flavobacterium pectinovorum</i> , <i>Flavobacterium sp. CS100</i>	97.72	Bacteroidetes Flavobacteria Flavobacteriales
OTU.131	3.07	3	<i>Flavobacterium fluvii</i> , <i>Flavobacterium bacterium HMD1033</i> , <i>Flavobacterium sp. HMD1001</i>	100.0	Bacteroidetes Flavobacteria Flavobacteriales
OTU.3540	2.52	3	<i>Flavobacterium terrigena</i>	99.54	Bacteroidetes Flavobacteria Flavobacteriales
OTU.107	2.25	3	<i>Flavobacterium sp. 15C3</i> , <i>Flavobacterium banpakuense</i>	99.54	Bacteroidetes Flavobacteria Flavobacteriales
OTU.277	3.52	3	<i>Solibius ginsengiterrae</i>	95.43	Bacteroidetes Sphingobacteriia Sphingobacteriales
OTU.183	3.31	3	No hits of at least 90% identity	89.5	Bacteroidetes Sphingobacteriia Sphingobacteriales
OTU.5906	3.16	3	<i>Terrimonas sp. M-8</i>	96.8	Bacteroidetes Sphingobacteriia Sphingobacteriales
OTU.360	2.98	3	<i>Flavisolibacter ginsengisoli</i>	95.0	Bacteroidetes Sphingobacteriia Sphingobacteriales

Table S2 – continued from previous page

OTU ID	Fold change	Day	Top BLAST hits	BLAST %ID	Phylum;Class;Order
OTU.369	5.05	1	<i>Paenibacillus sp. D75,</i> <i>Paenibacillus glycansilyticus</i>	100.0	<i>Firmicutes Bacilli Bacillales</i>
OTU.267	4.97	1	<i>Paenibacillus pabuli,</i> <i>Paenibacillus tundrae,</i> <i>Paenibacillus taichungensis,</i> <i>Paenibacillus xylanexedens,</i> <i>Paenibacillus xylanilyticus</i>	100.0	<i>Firmicutes Bacilli Bacillales</i>
OTU.1040	4.78	1	<i>Paenibacillus daejeonensis</i>	100.0	<i>Firmicutes Bacilli Bacillales</i>
OTU.57	4.39	1	<i>Paenibacillus castaneae</i>	98.62	<i>Firmicutes Bacilli Bacillales</i>
OTU.394	4.06	1	<i>Paenibacillus pocheonensis</i>	100.0	<i>Firmicutes Bacilli Bacillales</i>
OTU.319	3.98	1	<i>Paenibacillus xinjiangensis</i>	97.25	<i>Firmicutes Bacilli Bacillales</i>
OTU.5603	3.96	1	<i>Paenibacillus uliginis</i>	100.0	<i>Firmicutes Bacilli Bacillales</i>
OTU.1069	3.85	1	<i>Paenibacillus terrigena</i>	100.0	<i>Firmicutes Bacilli Bacillales</i>
OTU.843	3.62	1	<i>Paenibacillus agarexedens</i>	100.0	<i>Firmicutes Bacilli Bacillales</i>
OTU.2040	2.91	1	<i>Paenibacillus pectinilyticus</i>	100.0	<i>Firmicutes Bacilli Bacillales</i>
OTU.3	2.61	1	[<i>Brevibacterium</i>] <i>frigoritolerans</i> , <i>Bacillus sp. LMG 20238</i> , <i>Bacillus coahuilensis m4-4</i> , <i>Bacillus simplex</i>	100.0	<i>Firmicutes Bacilli Bacillales</i>
OTU.335	2.53	1	<i>Paenibacillus thailandensis</i>	98.17	<i>Firmicutes Bacilli Bacillales</i>
OTU.3507	2.36	1	<i>Bacillus spp.</i>	98.63	<i>Firmicutes Bacilli Bacillales</i>
OTU.8	2.26	1	<i>Bacillus niaci</i>	100.0	<i>Firmicutes Bacilli Bacillales</i>
OTU.4743	2.24	1	<i>Lysinibacillus fusiformis</i> , <i>Lysinibacillus sphaericus</i>	99.09	<i>Firmicutes Bacilli Bacillales</i>
OTU.9	2.04	1	<i>Bacillus megaterium</i> , <i>Bacillus flexus</i>	100.0	<i>Firmicutes Bacilli Bacillales</i>
OTU.22	2.8	7	<i>Paracoccus sp. NB88</i>	99.09	<i>Proteobacteria Alphaproteobacteria Rhodobacterales</i>
OTU.5	3.69	7	<i>Delftia tsuruhatensis</i> , <i>Delftia lacustris</i>	100.0	<i>Proteobacteria Betaproteobacteria Burkholderiales</i>
OTU.346	3.44	3	<i>Pseudoduganella violaceinigra</i>	99.54	<i>Proteobacteria Betaproteobacteria Burkholderiales</i>
OTU.32	3.0	3	<i>Sandaracinus amyloyticus</i>	94.98	<i>Proteobacteria Deltaproteobacteria Myxococcales</i>
OTU.68	3.74	7	<i>Shigella flexneri</i> , <i>Escherichia fergusonii</i> , <i>Escherichia coli</i> , <i>Shigella sonnei</i>	100.0	<i>Proteobacteria Gammaproteobacteria Enterobacteriales</i>
OTU.290	3.59	1	<i>Pantoea spp.</i> , <i>Kluyvera spp.</i> , <i>Klebsiella spp.</i> , <i>Erwinia spp.</i> , <i>Enterobacter spp.</i> , <i>Buttiauxella spp.</i>	100.0	<i>Proteobacteria Gammaproteobacteria Enterobacteriales</i>
OTU.11	5.25	7	<i>Stenotrophomonas pavani</i> , <i>Stenotrophomonas maltophilia</i> , <i>Pseudomonas geniculata</i>	99.54	<i>Proteobacteria Gammaproteobacteria Xanthomonadales</i>
OTU.48	2.99	1	<i>Aeromonas spp.</i>	100.0	<i>Proteobacteria Gammaproteobacteria aaa34a10</i>
OTU.241	3.38	3	No hits of at least 90% identity	87.73	<i>Verrucomicrobia Spartobacteria Chthoniobacteriales</i>

^a Maximum observed \log_2 of fold change.^b Day of maximum fold change.